

STRONTIUM UNDER HIGH PRESSURE AND DIFFERENT TEMPERATURE CONDITIONS: A MOLECULAR DYNAMICS SIMULATION STUDY

Murat Celtek¹, Unal Domekeli², Sedat Sengul²

¹Faculty of Education, Trakya University, 22030, Edirne – TURKEY

²Dept. of Physics, Trakya University, 22030, Edirne – TURKEY

Abstract

To investigate the effect of pressure applied during the heating process on the melting point and atomic structure of fcc strontium, we applied it by varying the pressure from 0 GPa to 8 GPa. Interactions between strontium atoms are described by the embedded atom method potential, which is widely used for metallic systems and shared by Sheng. Molecular dynamics simulations were performed with DLPOLY 2.0 open-source package program. For the results obtained under 0 GPa, the melting point, pair distribution function, and structure factor show good agreement with the experimental results. On the other hand, it was observed that fcc strontium made a first-order solid-liquid phase transition at higher temperatures with increasing pressure. Interestingly, with the effect of increasing pressure, abnormal behavior was observed in the volume-temperature curves. From the results of the pair distribution function and the pair analysis technique, it was observed that a solid-solid phase transition occurred in the system during the heating process. We hope that the results will add to the literature in understanding the structure of fcc strontium under high-pressure and high-temperature conditions.

Keywords: Strontium, High-pressure, Melting point, Atomic simulations, embedded atom method

INTRODUCTION

Molecular dynamics (MD) simulations have become a powerful tool to study many physical and mechanical properties of systems under conditions such as high pressure (HP) and high temperature in fields such as physics, biophysics, chemistry, and materials science due to increased computational power and software availability. MD simulations are often used in conjunction with a wide variety of experimental techniques such as X-ray crystallography, neutron diffraction, cryoelectron microscopy, nuclear magnetic resonance, electron paramagnetic resonance, and Forster resonance energy transfer. MD simulations have great advantages over experimental conditions and are an effective method for studying the physical motions of atoms and molecules. As it is known, a good understanding of the physical properties of metals and their alloys is of great importance in the advancement of technology and new developments in many fields. One of the most important studies on

metals and their alloys is the examination of the physical behavior of the material during the heat treatment under different conditions [1–3]. This study was carried out on the element strontium (Sr), which we have heard very little about, but which is widely used in medicine and fireworks and is abundant in the earth's crust, and has a face-centered cubic (fcc) structure. Throughout all MD simulations performed here, the atomic interactions between Sr atoms have been described by the embedded atom method (EAM) potentials, which are widely used in the literature for metals and their alloys. The melting points of the systems heated under different pressures were determined by using curves such as volume-temperature and energy-temperature. Apart from these, solid-liquid and solid-solid phase transitions are discussed over the results of the pair distribution function (PDF or $g(r)$) and the pair analysis (PA) technique [4]. In the following sections, theoretical information about these methods and the results obtained from them will be presented in detail.

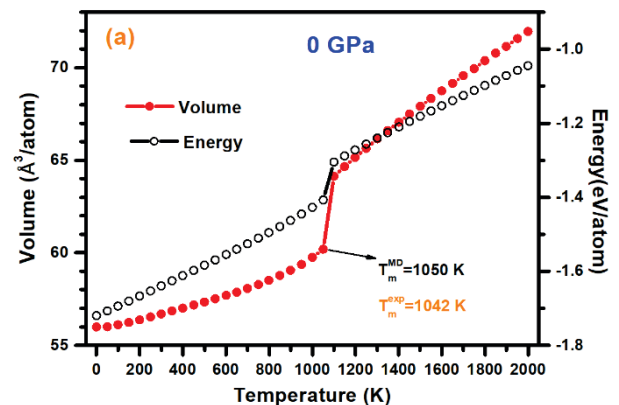
EXPOSITION

The analytical form of the EAM potential is defined as:

$$E_i = F_\alpha \left[\sum_{j \neq i} \rho_{\alpha\beta}(r_{ij}) \right] + \frac{1}{2} \sum_{j \neq i} \phi_{\alpha\beta}(r_{ij}) \quad (1)$$

where $\phi_{\alpha\beta}(r_{ij})$ denotes the pair interaction energy between atoms i and j . α and β are the element types of i and j atoms. F_α is the embedding energy and it depends on the atomic electron density (ρ). In our study, the data produced by Sheng and shared on his own web page were used as EAM potential. All MD simulations were carried out with DLPOLY 2.0 open source code [5], which is popular among simulation packages. The experimental lattice parameter ($a=6.08 \text{ \AA}$) [6] of Sr was used to construct the simulation box and the dispersion of atoms was structured in accordance with the fcc structure. The cubic cell contains 13500 Sr atoms ($15 \times 15 \times 15 \times 4$). A canonical ensemble with a Berendsen thermostat and barostat was used to control temperature and pressure. Periodic boundary conditions were applied along all three directions of the box in the simulations. The time step was set to 1 fs. Newton's equations of motion were integrated numerically using the leapfrog Verlet algorithm. To remove the accumulated stress on the system, we first heated the system to 100 K under 0 GPa and then cooled it back to 0 K. Thus, using these initial conditions for all pressures, the system was heated under different pressures, starting from 0 K up to 2000 K with 50 K temperature steps. The total energy per atom (E-T) and volume curves (V-T) obtained from the EAM-MD simulations during heat treatment under different pressures (0, 2, 4, 6 and 8 GPa) are shown in Figure 1 (a-e) as a function of temperature. As seen in Figure 1(a), the behavior of the E-T and V-T curves obtained for 0 GPa is similar. While a linear increase in V-T (or E-T) is observed from low temperatures, a sudden jump appears between 1050-1100 K, which is an indication that the system has made a first-order phase transition (Solid-Liquid). In addition, values such as lattice parameter ($a_{\text{latt.}}^{\text{MD}} = 6.08 \text{ \AA}$ and $a_{\text{latt.}}^{\text{exp}} = 6.08 \text{ \AA}$), cohesive energy ($E_{\text{Coh.}}^{\text{MD}} = -1.72 \text{ eV/atom}$ and $E_{\text{Coh.}}^{\text{exp}} = -1.72 \text{ eV/atom}$) and melting point ($T_m^{\text{MD}} =$

1050 K and $T_m^{\text{exp}} = 1042 \text{ K}$) [7] determined from the EAM potential for Sr under 0 GPa are in excellent agreement with the experimental results in the literature [6]. Consistent with the basic thermodynamic theory, the average energy of the atoms increases and the average atomic volume decreases under the influence of the residual pressure (see Figure 1(a-e)). However, different (or abnormal) behaviors were observed in V-T values with increasing pressure. Moreover, in contrast to the volume increase during the heating process under pressures of 2-8 GPa, volume contraction is observed, which is observed at different temperature values for different pressures. Various research groups have previously reported results similar to those we observed for metallic systems cooled under different pressures [3, 8, 9]. This particular observation for V-T values can be well explained by the Clausius-Clapeyron relationship [10]. Interestingly, this behavior observed in V-T curves is somewhat different in E-T curves. Contrary to V-T, in the E-T curves obtained for 2 and 4 GPa pressures, no sudden changes are observed until the melting point, while in the E-T curves obtained for 6 and 8 GPa pressures, sudden changes are observed at the same temperature points as in the V-T curves. Well, is it possible to explain the contraction observed in the volume with the local structure based on the current findings? Or did another phase transition such as solid-solid occur in the system during heat treatment? In order to give appropriate answers to these questions, we will focus on the structural evolution that occurs in the system during the heating process under different pressures in the following sections.



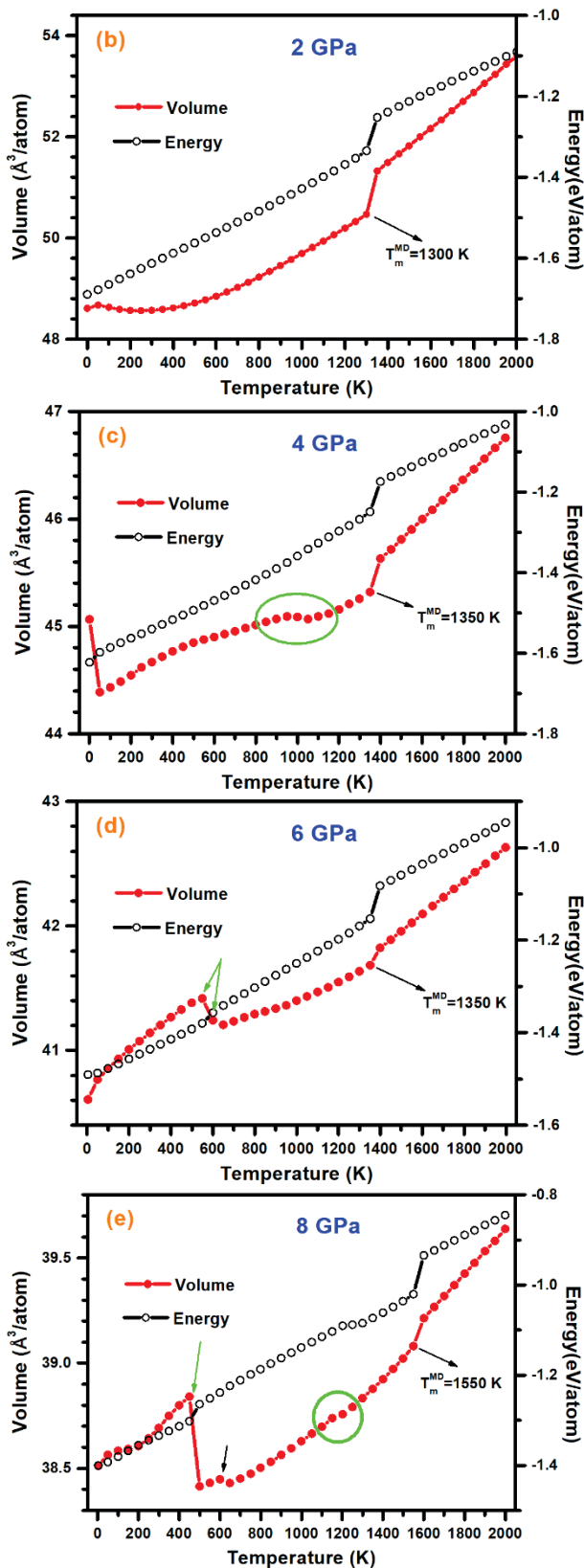


Fig. 1. Temperature-dependent evolution of volume and energy curves obtained under (a) 0 GPa, (b) 2 GPa, (c) 4 GPa, (d) 6 GPa and (e) 8 GPa pressure.

The $g(r)$ function, which is of great importance in determining the structural properties of substances, provides very useful information

about the structural evolution of the system under different conditions, as it depends on the phases of matter, the arrangement of atoms in space and the distance relations between atoms. The $g(r)$ function used in MD simulations is defined as follows [11]:

$$g(r) = \frac{V}{N^2} \left\langle \sum_i^N \sum_{j \neq i}^N \delta(r - r_{ij}) \right\rangle \quad (2)$$

where N represents the number of atoms placed in the simulation box, and V represents the volume of the simulation box formed by these atoms.

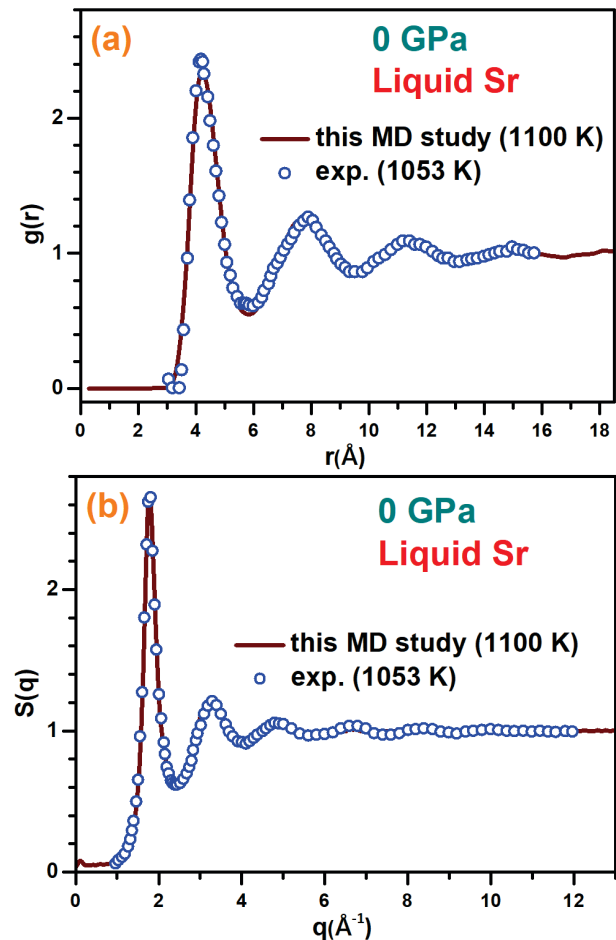


Fig. 2. Comparison of (a) $g(r)$ and (b) $S(q)$ calculated for liquid Sr with experimental results [12].

The $g(r)$ and $S(q)$ curves calculated from the EAM-MD simulations for liquid Sr under 0 GPa pressure are presented comparatively in Figure 2 (a-b), together with the experimental results [12]. Both curves show excellent agreement with their experimental curves. All these findings indicate that the selected EAM potential data are successful in explaining the physical parameters and structural properties of Sr at both low and high temperatures. All this is of great importance for the reliability of the

results obtained under different pressures. Moreover, in order to see the effect of the pressure more clearly, the $g(r)$'s calculated at 2000 K for all pressure values are plotted together in Figure 3. As expected, with increasing pressure, the main peaks of the $g(r)$ curves shift towards smaller r values, while the peak heights increase slightly.

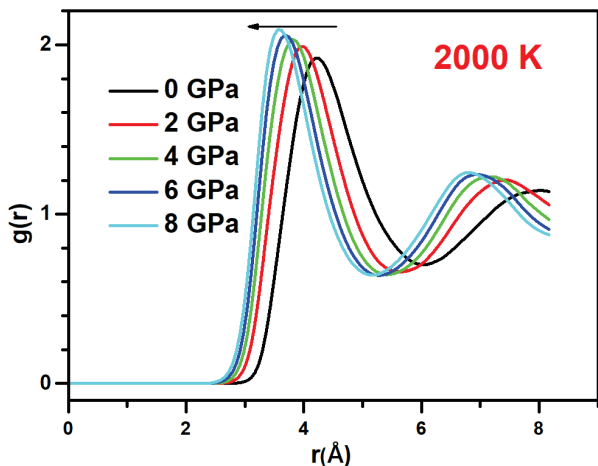


Fig. 3. $g(r)$ curves calculated for different pressures at 2000 K.

In order to answer the above questions and avoid repetition, the sudden change points observed in the V-T curves of 4 GPa and 8 GPa and the $g(r)$ curves around melting points are shown together in Figure 4. It is seen from the characteristic features of the peaks of the $g(r)$ curves around the melting points for both pressures that the system makes a solid-liquid phase transition. There is a sudden decrease in volume around 1000 K in the V-T curve obtained for 4 GPa, and when the $g(r)$ curves calculated for these points are examined, no evidence of solid-solid phase transition was found. However, when the $g(r)$'s calculated for 450 K and 500 K under 8 GPa are compared, it is clear that there is a significant difference between them, which shows us that solid-solid phase transition occurs in the system between these points. From the available $g(r)$ -curves it is unlikely to tell what kind of crystal-like structure the fcc-like crystal structure is transformed into. In order to make a more detailed comment, it is necessary to get support from different analysis methods. In our study, we chose the PA technique to explain this process and included the results about it. In this technique (or the Honeycutt-Andersen method), the local structure (ijkl) in the atomic

cluster is defined by four basic indices. Please see Ref [13–15]s for more detailed information.

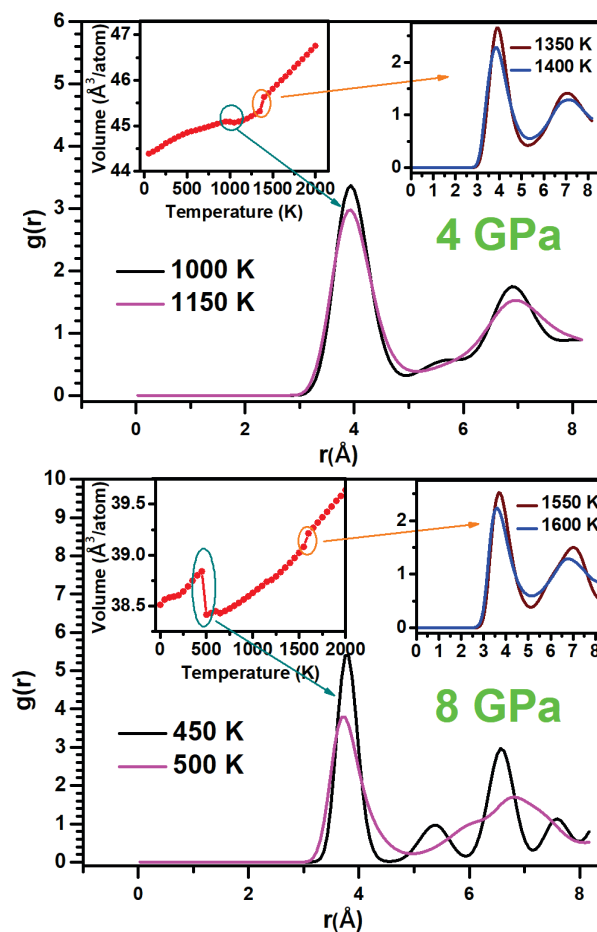


Fig. 4. Calculated $g(r)$'s for different temperature under 4 GPa and 8 GPa pressure.

The temperature-dependent evolution of those most commonly found in the system among the bonded pairs obtained from the PA analysis technique under three different pressures (0, 4 and 8 GPa) is shown in Figure 5. As seen in Figure 5(a), the fraction of 1421 bonded pairs representing the fcc crystalline structure gradually decreases in the system heated under 0 GPa pressure, while the fraction of 1541 and 1431 bonded pairs, which are more common in liquid and amorphous structures, gradually increases. Finally, a sharp change in these curves is observed at the melting point. For the system heated under a pressure of 4 GPa, the fraction of 1421 bonded pairs is around 100% at 0 K, but interestingly, their fraction drops sharply by around 30% when the temperature is increased to 50 K. From 100 K their fraction increases and reaches its maximum value at around 500 K, and finally their fraction gradually decreases again until around the

melting point. The results in Figure 5(b) show that the applied pressure and increasing temperature affect the crystalline order of the system and as a result, some of the 1421 bonded pairs transform into other clusters. However, despite all this, the dominance of 1421 bonded pairs continues until around the melting point, which is proof that the solid-solid phase transition does not occur in the system. These findings support the other results discussed above. Finally, we obtained findings showing significant changes in the microstructure of fcc Sr heated under 8 GPa pressure and plotted them in Figure 5(c). When the temperature is increased from 0 K to 100 K, the fraction of 1421 bonded pairs decreases from 100% to around 80%, and then increases to around 95% of their fraction. A sudden decrease is observed in the fraction of 1421 bonded pairs in the region between 450 K-500 K, while an increase is observed in the fraction of 1441 and 1661 bonded pairs representing bcc crystal structures and 1541 and 1431 bonded pairs representing distorted icosahedra structures. To provide a better overview of the solid-solid phase transition observed here, we have classified the bonded pairs as bcc (1441+1661), hcp+fcc (1421+1422), icos (1431+1541+1551), and other types and presented in the inset of Figure 5(c). Between 450K and 500K, the fraction of bcc type clusters increases to ~52% and the fraction of icos types to ~27%, while the fraction of fcc+hcp types decreases to around ~19%. The results show that fcc Sr undergoes a solid-solid phase transition in this range, but a polycrystalline structure is formed rather than a transition from fcc structure to single bcc crystal order. The results of the present study show that the microstructure and many structural properties of fcc Sr change significantly under conditions such as HP and high temperature during heat treatment. We believe that the results will guide further studies to understand the structural properties of Sr nanoparticles and their mechanical properties under tension conditions. Figure 6 depicts the distribution of fcc, bcc and other types in the solid-solid phase transition occurring between 450-500 K under 8 GPa. At 450 K, the atoms that make up the system appear to have a distribution specific to fcc structures, while bcc

and other types crystal structures are very rare. Moreover, when the temperature is increased by 500 K, a significant decrease is observed in the number of fcc clusters, while a significant increase is observed in the number of bcc and other clusters. This supports the results obtained with different analyzes above and gives us a visual view.

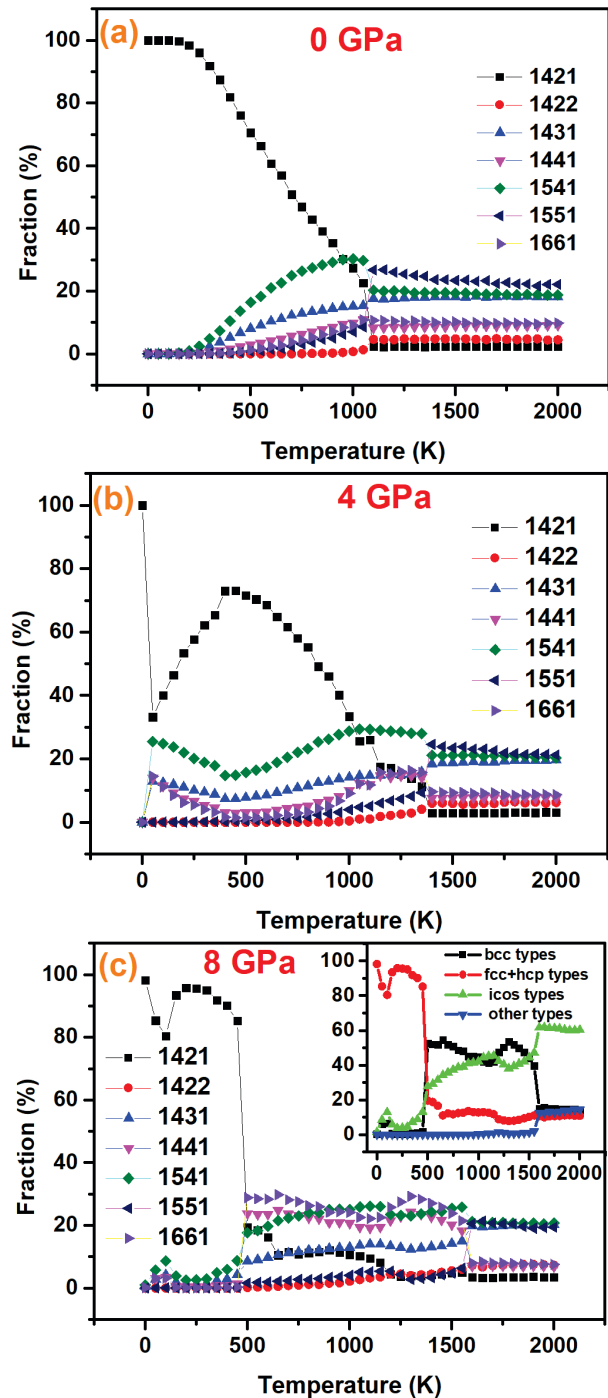


Fig. 5. Temperature-dependent fractions of the most common PA bonded pairs obtained under pressures of (a) 0 GPa, (b) 4 GPa and (c) 8 GPa..

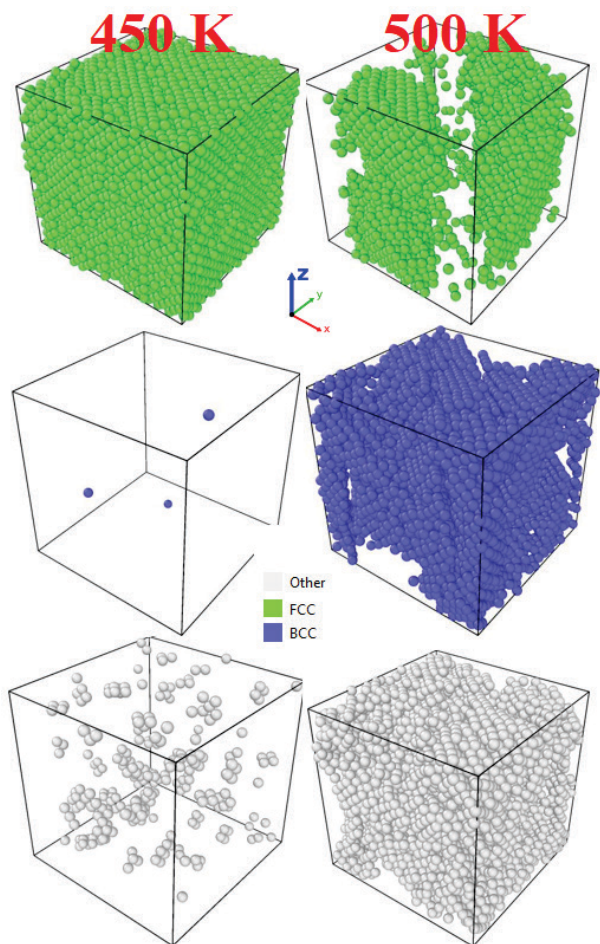


Fig. 6. Distribution of fcc, bcc and other types at 450 K and 500 K under 8 GPa.

CONCLUSION

The melting process and microstructure evolution of fcc Sr under different pressures have been investigated by MD simulations using EAM potentials. We observed that the EAM potential predicted the lattice parameter, cohesive energy and melting temperature of the element Sr with high accuracy. Also, $g(r)$ and $S(q)$ calculated for liquid Sr showed excellent agreement with the experimental results. The melting point increased with increasing pressure and significant changes were observed in the microstructure of the system. Solid-solid phase transition occurred between 450-500 K (500-550 K) under 8 GPa (6 GPa). The results of the PA analysis technique showed that most of the atoms with the fcc crystal arrangement in the phase transition have been oriented towards the bcc crystal arrangement.

REFERENCE

[1] Guder V, Sengul S, Celtek M, et al. Pressure dependent evolution of microstructures in

- Pd80Si20 bulk metallic glass. *J Non Cryst Solids* 2022; 576: 121290.
- [2] Celtek M. Atomic structure of Cu60Ti20Zr20 metallic glass under high pressures. *Intermetallics* 2022; 143: 107493.
- [3] Li C, Luo Z, Tian Z, et al. The concealed solid-solid structural phase transition of Fe70Ni10Cr20 under high pressure. *Mater Today Commun* 2022; 104499.
- [4] Celik FA. Pressure and cooling rate effect on polyhedron clusters in Cu–Al alloy by using molecular dynamics simulation. *Phys B Condens Matter* 2014; 450: 71–76.
- [5] Smith W, Forester TR. DL_POLY_2.0: A general-purpose parallel molecular dynamics simulation package. *J Mol Graph* 1996; 14: 136–141.
- [6] Kittel C. *Introduction to Solid State Physics*. New York: John Wiley & Sons Inc., 1986.
- [7] Celtek M, Domekeli U, Sengul S. Investigation of first order phase transition process of strontium during heating with molecular dynamics simulations using different potentials. In: *International Scientific Conference. Bulgaria/Gabrovo, 2021*, pp. 259–264.
- [8] Sengul S, Celtek M, Domekeli U. The structural evolution and abnormal bonding ways of the Zr80Pt20 metallic liquid during rapid solidification under high pressure. *Comput Mater Sci* 2020; 172: 109327.
- [9] Kang H, Ye X, Wang J, et al. Abnormal bonding ways in Zr50Cu50 metallic glass under high pressures. *J Alloys Compd* 2019; 780: 512–517.
- [10] Kenneth W. *Generalized Thermodynamic Relationships*. New York, 1988.
- [11] Yildiz AK, Celik FA. Atomic concentration effect on thermal properties during solidification of Pt-Rh alloy: A molecular dynamics simulation. *J Cryst Growth* 2017; 463: 194–200.
- [12] Waseda Y. *The Structure of Non-Crystalline Materials-Liquids and Amorphous Solids*. New York: London: McGraw-Hill, 1981.
- [13] Celtek M, Sengul S, Domekeli U, et al. Dynamical and structural properties of metallic liquid and glass Zr48Cu36Ag8Al8 alloy studied by molecular dynamics simulation. *J Non Cryst Solids* 2021; 566: 120890.
- [14] Honeycutt JD, Andersen HC. Molecular Dynamics Study of Melting and Freezing of Small Lennard-Jones Clusters. *J Phys Chem* 1987; 91: 4950–4963.
- [15] Celtek M, Domekeli U, Sengul S, et al. Effects of Ag or Al addition to CuZr-based metallic alloys on glass formation and structural evolution: a molecular dynamics simulation study. *Intermetallics* 2021; 128: 107023.